Postnatal activation of hypoxia pathway disrupts β-cell functional maturation

Juxiang Yang[1*], Batoul Hammoud[1*], Abigail Ridler[1], Amanda M. Ackermann[1,2], Kyoung-Jae Won[3], Toshinori Hoshi[4], Charles A. Stanley[1,2], and Diana E. Stanescu[1,2]

[1] Division of Endocrinology and Diabetes, The Children's Hospital of Philadelphia, Philadelphia, PA

[2] Department of Pediatrics, Perelman School of Medicine, University of Pennsylvania, Philadelphia, PA

[3] Biotech Research & Innovation Centre, University of Copenhagen, Denmark

[4] Department of Physiology, Perelman School of Medicine, University of Pennsylvania, Philadelphia, PA

*Co-first authors

Word count: 5094

Number of figures: 5 main figures, 5 supplemental figures

Key words: β-cell, hypoxia, threshold

Disclosure statement: all authors have nothing to disclose

Abstract:

Objective: Hypoxic injuries occurring during the perinatal period can lead to persistent hyperinsulinism and profound hypoglycemia in newborns. We studied the impact of hypoxia-inducible pathway on the postnatal β-cell function.

Methods: Rat pups were treated daily between postnatal day (P)7 to P10 with adaptaquin (AQ), an inhibitor of prolyl hydroxylases, leading to stabilization of hypoxia-inducible factor 1A (HIF1A). In parallel, mouse pups were placed in a hypoxic chamber between embryonic day (E)19 to P6. Dynamic insulin secretion was assessed in both models by islet perifusions. Changes in gene expression were assessed by whole-islet RNA sequencing.

Results: AQ-treated rat pups and hypoxic mouse pups were hypoglycemic and had higher levels of serum insulin. The AQ-/hypoxia-treated islets showed a decreased glucose threshold for insulin secretion compared to controls, indicative of a delay in β-cell postnatal functional maturation. Islet morphometric analysis in the AQ-treated pups showed an increase in insulin area per pancreas, but no change in the number of islets or in the number of β-cells per islet, consistent with a higher average size of β-cells. Differential transcriptomic analysis showed upregulation of the expected HIF1A target genes. AQ-treated rat pups had decreased expression of cell cycle genes and decreased numbers of proliferating β-cells.

Conclusion: We showed that hypoxia and pharmacologic activation of the hypoxia inducible pathway in early postnatal period leads to hyperinsulinism, due to the persistence of a low glucose threshold for insulin secretion. This exaggerated activation of hypoxia pathway also decreased early postnatal β-cell proliferation, suggesting it can impact adult β-cell mass and diabetes risk.

Introduction:

Perinatal stress and birth asphyxia lead to profound and prolonged hypoglycemia due to increased insulin secretion from β-cells and is clinically termed perinatal stress-induced hyperinsulinism. Approximately 8-10% of infants admitted to a neonatal intensive care unit are diagnosed with this condition, which can persist for several months (1-4). Afflicted babies are at very high risk of developing severe hypoglycemia leading to hypoglycemic seizures and life-long neurologic impact (5). Most cases respond well to treatment with the K_{ATP} channel agonist diazoxide to suppress insulin secretion, but some require high intravenous or enteral glucose support for a prolonged period after birth(4). The underlying mechanism for the increased insulin secretion in perinatal stress-induced hyperinsulinism is unknown. This form of hyperinsulinism has been hypothesized to represent a prolongation of the transitional neonatal hypoglycemia occurring in healthy newborns (3).

Activation of hypoxia-inducible pathway by perinatal stress is proposed as a potential mechanism affecting β-cell function (3). This cellular pathway helps cells adapt to hypoxic conditions and is mediated by the hypoxia-inducible factor (HIF1) complex (6). The α subunit (HIF1A) is oxygen sensitive. Under normoxia HIF1A is hydroxylated by prolyl hydroxylases (PHDs) and associated with the von Hippel Lindau factor (VHL), facilitating proteasomal degradation (7). In contrast, under hypoxia HIF1A is not readily degraded and binds to its partner – the hypoxia-inducible factor β subunit (HIF1B/ARNT). The HIF1 dimeric complex then translocates into the nucleus, where it binds to hypoxia response elements (HRE) in promoter and enhancer regions, regulating a multitude of cellular process aimed at cell survival.

Since its discovery, the HIF1A pathway has been explored for its potential to impact pancreatic endocrine development and adult islet function. Due to differences in oxygen tension and vascularization, pancreatic HIF1A levels are high during gestation, but decrease greatly after birth (8). Furthermore, activation of the hypoxia pathway in rodents is negatively correlated with β-cell maturation in the immediate postnatal period (9). Both pharmacologic and O_2-

mediated stabilization of HIF1A promoting the dimeric complex formation during intrauterine period lead to decreased endocrine differentiation (10). Loss of VHL and subsequent HIF1A stabilization in mice in pancreatic endocrine progenitors result in profound hypoglycemia leading to death in the majority of pups prior to weaning.(11) However, loss of VHL in differentiated β cells can have a normal or slightly lower plasma glucose and a mild impairment in glucose tolerance (12-15).

We hypothesize that activation of the hypoxia inducible pathway in the perinatal period leads to hyperinsulinism by delaying postnatal functional maturation of β-cells. We show that in rodents hypoxia and pharmacologic inhibition of prolyl hydroxylases lead to hypoglycemia and hyperinsulinism due to the persistence of a lower glucose threshold for insulin secretion. In addition to the hyperinsulinism phenotype, rat pups with pharmacologic activation of HIF1A pathway have dramatic changes in whole islet transcriptomes and decreased β-cell proliferation.

Methods:

1. Animals:

Animal experiments were performed in rats and mice according to the IACUC-approved protocol at The Children's Hospital of Philadelphia. Pregnant Sprague Dawley rats at embryonic day (e)15 or e17 and pregnant CD1 mice at e15 were purchased from Charles River Laboratories (Wilmington, MA). Dams and pups were housed together in AAALC-approved rodent colony. Due to the small size of the pancreas from both the rat and the mouse pups, male and female pups were batched together for measurements.

For administration of adaptaquin (AQ), P3 and P7 rat pups were injected daily for 4 days with 40-60 mg/kg body weight (first 2 days 40 mg/kg followed by 2 days of 60 mg/kg) of AQ (Sigma or Cayman Chemical) resuspended in DMSO. Control pups of the same age were injected with DMSO control solution. Pups were euthanized and then blood and pancreata were collected at day P7 or P11 for islet isolation and functional analysis.

For the hypoxia experiments, pregnant CD1 mice were placed in a hypoxic chamber (Biospherix, NY) with 10% O_2 at e19, by displacing O_2 with N_2. Pups were delivered in hypoxic conditions during the first 24 hrs in the hypoxic chamber. Dam and pups were monitored for signs of distress. They were kept in hypoxia chamber until P6, when pups were euthanized immediately after removal from the chamber. Blood and pancreata were collected for islet isolation and functional analysis under normoxic conditions. Control dams at the same gestational age were kept under ambient normoxic conditions.

For BrdU staining, the solution of BrdU (10 mg/ml) was dissolved in PBS and was protected from light. Rats were weighted, injected intraperitoneally with 100 mg/kg BrdU, and scarified 24 hrs after the injection.

2. Islet isolation and perifusions

Islet isolation and perifusions were performed as previously described by our group (16). In brief, islets were isolated from control/AQ-treated rat pups and from normoxic/hypoxic mouse pups. Islets, 200-250, were batched together from 2-3 rat pups or from 3-5 mouse pups. Perifusions were performed within 2 hrs after islet isolations, with increasing glucose concentrations in the perifusion media from 3 to 25 mM. Samples were collected every min for insulin assay using Insulin High Range Kits (Cisbio Assays, Bedford, MA) following the manufacturer's instructions.

3. Whole islet RNAseq and RNA qPCR

Total islet RNA was prepared using Qiagen RNeasy Mini Kit (Qiagen, Germantown, MD) following the manufacturer's protocol, from batched islets from control and AQ-treated P11 pups. For the whole islet RNAseq, 3 control islet preparations and 2 AQ islet preparations were sent to Novogene (Beijing, China) for library preparation, sequencing and analysis. Novogene workflow consists of the following steps: sample quality control, library preparation and library quality control, sequencing, data quality control, and bioinformatic analysis. Sequenced reads were aligned to the *Rattus norvegicus* genome, with total mapping rate >75% for all samples. Differential expression analysis of control vs. AQ-treated islets was performed using the DESeq2 R package(17). Gene ontology analysis of differentially expressed genes was performed in Ingenuity IPA (Qiagen, Germantown, MD).

For individual targets, total RNA was reverse transcribed using random primers and High-Capacity cDNA Reverse Transcription kit (Applied Biosystems, Waltham, MA). Quantitative PCR (QuantStudio 6, Applied Biosystems, Waltham, MA) was used to measure gene expression levels and normalized to the housekeeping gene hypoxanthine guanine phosphoribosyl transferase (*Hprt*),for the rat data, and β actin for the mouse data. The primer sequences used are listed in Supplemental Table 1.

4. Glucose and hormone assays

Plasma glucose levels were measured from tail blood using a Contour Next glucose meter (Ascensia Diabetes Care, NJ). For serum insulin and glucagon measurements, blood was collected immediately after euthanasia into heparinized microvette CB300 (Sarstesdt, Newtown, NC) and centrifuged at 4 °C for 5 min at 800 × *g*. The plasma supernatant was transferred to a fresh 2 mL tube and stored at −80 °C. Plasma insulin and glucagon were detected with an ELISA kit (Cisbio US Inc, Bedford, MA and Mercodia AB, Uppsala, Sweden, respectively). For insulin or glucagon content, whole pancreas was collected the sonicated in acid ethanol 0.18 M HCl in 70% ethanol. The sonicate was placed at 4 °C for 12 hrs. Before hormones analysis, the samples were vortexed to avoid adding cellular debris and then diluted 1000 times.

7. Immunostaining

Pancreas tissues were dissected, immediately fixed in 4% paraformaldehyde overnight, and washed with PBS 3 times. Pancreas tissues were prepared for either frozen or for paraffin sections. For frozen/cryosections, pancreas samples were embedded in optimal cutting temperature compound (Tissue-Tek O.C.T. Compound, Sakura Finetek, Tokyo, Japan) and stored at −80 °C until sectioning on cryostat. For paraffin sections, the tissue was sequentially dehydrated with 40, 70, 80, 95, and 100% ethanol, rinsed twice with xylene, and then embedded in paraffin. Frozen pancreas tissues were cut into 10-µm thickness sections and paraffin-embedded tissues were sectioned at 6 µm thickness. Paraffin sections were heated, dewaxed with xylene, rehydrated using an alcohol gradient, and washed with PBS. The slides were treated with 10 mM sodium citrate (pH 6) with 0.05% Tween 20 at 90–95 °C for 2 hrs. Both frozen and paraffin sections were penetrated with 0.5% Triton X-100 (Sigma, USA) at room temperature for 15 min, blocked with 5% normal donkey serum (Jackson ImmunoReseach, West Grove, PA) at 37 °C for 1 h, and incubated with the primary antibody at 4 °C overnight. Primary antibodies are listed in Supplemental Table 2. The slides were treated with the

secondary antibody at 37 °C for 60 min and mounted with DAPI. Fluorescence images were visualized on Olympus IX73. When expression levels of proteins between samples were compared, images were captured utilizing identical optical settings. The images were captured and analyzed using MetaMorph version 7.1 (Molecular Devices, Sunnyvale, CA). The insulin-containing and glucagon-containing areas were estimated from the measured fluorescence as the ratio between total amount of measured fluorescence for the insulin/glucagon staining and the number of pancreatic DAPI+ nuclei in each section. The total pancreas area was measured as the total area of background fluorescence (in the Cy2 channel) for each section, using the same criteria for each section/slide. A total of 3-5 sections, at least 100 μm apart were counted for each animal. For the individual islet measurements, the numbers of α- and β-cells in each islet were counted, as well as the area of fluorescence corresponding to insulin/glucagon.

8. Statistical analysis

The results were evaluated with unpaired Welch t-tests or Wilcoxon-Mann-Whitney test and P values are reported solely as data sample descriptors. All tables and graphs were analyzed and constructed using GraphPad Prism v 7.0 software.

Results:

Activation of HIF1A pathway leads to hypoglycemia and hyperinsulinism

To evaluate the effect of hypoxia pathway activation on glucose homeostasis in the neonatal period, we treated neonatal rat pups with AQ, a hydroxy-quinoline inhibitor of PHDs (18). This leads to the stabilization of HIF1A and activation of the HIF1 pathway even in normoxia (19). Rat pups received AQ or vehicle solution once daily by subcutaneous injections from postnatal day (P) P7 to P10. At P11, islets from AQ-treated pups had overall higher levels fluorescence for HIF1A compared to the controls suggesting higher HIF1A protein levels (representative images in Fig. 1A). AQ-treated islets showed increased expression of classical HIF1A target genes, such as the glucose transporter GLUT2(*Slc2a2*), glucokinase (*Gck*), vascular endothelial growth factor (*Vegf*), and glycolytic enzymes (*Aldo, Pdk1, Pfk*)(Fig 1B).

The AQ-treated pups had a lower weight (Fig. 2A), while no feeding difficulties were noted by observation of the pups and their stomachs were filled with milk similarly to controls at the time of euthanasia. Plasma glucose was lower while serum insulin and glucagon were higher (Fig. 2B-D). The levels of plasma glucose and serum insulin were negatively correlated in the AQ-treated pups, while the glucose and serum glucagon levels not correlated (Fig. 2E-F). The glucose threshold for insulin secretion from AQ-treated islets was lower (5 mM) when compared to the control P11 pups (10 mM; Fig. 2G-H). The glucose threshold of P11 AQ-treated islets was identical to the threshold of P7 untreated islets that we reported previously (16). AQ treatment of younger rats (from P3 to P6) had a similar impact of glucose homeostasis (Suppl. Fig. 1). By P7, AQ-treated pups had a lower body weight, lower plasma glucose and higher serum insulin (Suppl. Fig 1A-C). The glucose threshold was similarly shifted left, although to a lesser extent, because the glucose threshold of the P7 control islets was already lower.

To test whether the observed changes were an overall consequence of activation of the HIF1A pathway or due to a HIF1-independent effect of AQ, we assessed glucose homeostasis in hypoxic neonatal mouse pups. These newborn mouse pups were kept in mild hypoxia (10%

FiO_2) for the first 6 days of life and developed a phenotype similar to the AQ-treated rat pups: a decrease in body weight, lower plasma glucose, higher serum insulin, and serum glucagon (Suppl. Fig 2A). Islets from hypoxic mice had a lower threshold for insulin secretion (3 mM) compared to normoxic mice (5 mM) (Suppl. Fig 2B). Hypoxic islets showed the expected upregulation of HIF1A target genes, such as *Gck, Vegf, Aldoa,* and *Pfk* (Suppl. Fig. 2C).

Together these findings suggest that activation of the HIF1A pathway in the early postnatal period, either by pharmacologic inhibition of PHDs or through hypoxia, delays the postnatal β-cell functional maturation of the glucose threshold for insulin secretion.

Activation of HIF1A by AQ leads to changes in islet morphology

To determine the changes in islet-cell composition triggered by HIF1A pathway activation, we analyzed the morphometric characteristics of islets from P11 control and AQ-treated rat pups. The AQ-treated pups had a greater median insulin+ area per pancreas compared to controls and a trend to a greater median glucagon+ area (Fig. 3A). At the islet level, we found both higher insulin and higher glucagon area per cell area when compared with control P11 (Fig. 3B-C). There was no difference in the number of β- or α-cells in each islet (Fig. 3D-E). There was also no difference in insulin content between the two groups (Fig. 3F). AQ-treated pups a had a lower glucagon content compared to controls (Fig. 3G), possibly due to persistent glucagon secretion in the setting of hypoglycemia. These finding suggest that HIF1A pathway activation leads to an increased size of α- and β-cells, without a change in islet cell composition.

Activation of HIF1A by AQ leads to changes in whole islet transcriptome

To further determine the changes in islet structure and function induced by HIF1A pathway activation, we performed differential transcriptomic analysis in whole islets from AQ-treated and control P11 pups. A total of 479 genes were upregulated and 616 genes were

downregulated in AQ-treated P11 pup islets compared to control (Suppl. Table 3). Gene ontology analysis showed changes in expression of several pathways associated with cell cycle regulation (Fig 4A). Specifically, "*nucleotide excision repair pathway*", "*mitotic roles of polo-like kinases*" and "*p53 signaling*" were shown to be upregulated, while "*G2/M checkpoint regulation*", "*role of CHK proteins in cell cycle checkpoint contro*l", "*cyclins and cell cycle regulation*" and "*pyrimidine de novo synthesis*" pathways were downregulated (Fig. 4A). In line with the activation of HIF1A pathway by AQ inhibition of PHDs, several other hypoxia- or HIF1A-regulated transcripts were found to be differentially expressed. Specifically, the EGF receptor ligand amphiregulin (*Areg*), hypoxia inducible factor 3α (*Hif3a*), the CCAAT/enhancer-binding protein delta (*Cepbd*), the peptidase trefoil factor 3 (*Tff3*) and the signal transducer and activator of transcription 3 (*Stat3*) were upregulated; the pancreatic stellate cell proteoglycan lumican (*Lum*) was downregulated (Suppl. Fig 3A) (20-25). Several β-cell associated factors were altered in the AQ-treated islets (Fig. 4B). The transcription factor *Sox17*, a known target of HIF1A and regulator of insulin secretion, was upregulated in the AQ-islets (26, 27). Another regulator of insulin gene - *Klf11*, as well as transcription factors important for β-cell development and function, *Nkx2-2* and *NKX6-1*, had similar increased expression in islets from AQ-treated pups (28-31). *FoxM1*, a transcription factor essential for β-cell postnatal proliferation, was downregulated in the AQ-islets (32) (Fig. 4B). Other islet specific transcripts, such as *Ins1*, *Ins2*, *MafA,* and *MafB*, were not differentially expressed (Suppl. Fig. 3B).

Activation of HIF1A by AQ blunts postnatal β-cell proliferation

We noted a significant change in cell cycle related genes in whole islets from AQ-treated and control P11 pups. We found a 40-80% downregulation in *Cdk1, Mki67, Top2a*, and several other proliferation-related transcripts (Fig. 5A). We further investigated the impact of activation of the HIF1a pathway on islet cell proliferation by two markers of cell proliferation, KI67 (Fig. 5B) and BrdU (Suppl. Fig. 4A), in AQ-treated and control P11 rat pups. We found that fewer β-cells

in the AQ-treated pups were labelled KI67 or BrdU in the AQ-treated pups (Fig. 5B and Suppl. Fig 4A, respectively). Upstream regulator analysis in Ingenuity IPA revealed that over 100 of the differentially expressed genes are targets of the transcription factor MYC or its target transcription factor E2F1 (Suppl. Fig. 4B). While *Myc* transcript level was not different in the AQ-treated islets (Fig. 5A), the expression of *E2f1* was reduced by 70% compared to control. This suggests that activation of the HIF1A pathway could lead to decreased β-cell proliferation through a MYC-E2F1-dependent mechanism, potentially through direct antagonism at MYC targets (33). This effect on islet cell replication, during a crucial period for establishing adult islet mass, suggests that a brief neonatal HIF1 pathway activation could impact adult β-cell mass and future glucose homeostasis.

Discussion:

Perinatal stress-induced hyperinsulinism is an important clinical problem affecting newborns, leading to short- and long-term health complications. We explored how activation of the hypoxia pathway in neonatal rodents parallels the clinical findings in this form of hyperinsulinism. Our results show that activation of the HIF1A pathway in neonatal islets leads to hypoglycemia and hyperinsulinism by delaying postnatal β-cell functional maturation. Islets from P11 rat pups treated with AQ maintain a lower glucose threshold for insulin secretion, a salient characteristic of embryonic/early neonatal islets(16, 34, 35). The AQ-treated islets contain larger β- and α- cells and have marked changes in their transcriptomic profile. In addition, AQ-treated islets have diminished β-cell proliferation, suggesting blunting of the postnatal proliferation peak and potentially decreasing adult β-cell mass.

Mice with the HIF1A pathway activated in pancreatic endocrine progenitors have severe neonatal hypoglycemia causing early postnatal death (11). This hypoglycemia was accompanied by a mild glucagon secretion defect at low glucose concentrations from an otherwise normal α-cell mass. These changes in glucagon secretion were postulated to explain the profound hypoglycemia (11). However, the observed decrease in glucagon secretion is surprising in view of the severity of hypoglycemia. In other mouse models, targeted loss of α-cells or impairment of glucagon signaling does not lead to such a hypoglycemia causing early mortality (36, 37). Our results here demonstrate that activation of the HIF1A pathway in neonatal pups leads to hypoglycemia due increased insulin secretion driven by a lower β-cell glucose threshold for insulin release. Hypoglycemic mice have higher serum glucagon levels, suggesting an α-cell defect causing hypoglycemia is not present.

An important question is whether the hyperinsulinism phenotype is a direct consequence of HIF1A pathway activation in islets or due to its impact on other systems, which could in turn affect β-cell function. Both our models involved whole-body activation of the HIF1A pathway, either pharmacologically or through whole-body hypoxia. The lower glucose threshold for insulin

secretion in *ex vivo* AQ-islets, hours after isolation from animals, suggests that a short-term hormonal factor is not responsible for the observed changes. We cannot fully rule out the contribution of other secreted factors driven by whole-body hypoxia, which could have a longer-term impact on β-cell function. However, the parallel between our findings and the severe hypoglycemia in pups with genetic activation of the HIF1A pathway in endocrine progenitor cells (11), places changes in β-cell function driven by HIF1A as the prime central mechanism leading to hyperinsulinism.

The underlying mechanism of the lower glucose threshold for insulin release has been studied by us and others in the context of the normal postnatal β-cell functional maturation (16, 38-41). We evaluated the islet mRNA expression of these previously proposed factors in rat pups with HIF1A pathway activation. Disallowed islet factors, such as *Slc16a1*(MCT1) and *Ldha*, or maturational factors such as *Syt4* did not have transcriptomic changes consistent with driving a lower glucose threshold. We found an increase expression of glucokinase (*Gck*), as well as increased expression of several channels and transporters (*Slc2a2, Fxyd2, Slc38a4*), which may be related to changes in threshold for GSIS. Overall, these broad transcriptional changes suggested that HIF1A pathway has a significant impact on islet cell transcriptome, affecting multiple functional related genes. These findings highlight the need for future experiments exploring the direct mechanism by which HIF1A pathway impacts the threshold for GSIS.

Our studies focused on assessing the impact of hypoxia/HIF1A pathway only in the early postnatal period. Clinically, only perinatal or very early postnatal hypoxic insults lead to hyperinsulinism and hypoglycemia. Hypoxic insults during adulthood, such as travel to high altitude or obstructive sleep apnea, are in contrast associated with hyperglycemia, impaired glucose tolerance and signs of metabolic syndrome (42, 43). In the adult hypoxic β-cell injury, a lower glucose threshold for GSIS may be masked by the effects of other antagonistic hormones, such as cortisol, glucagon or catecholamines. These hormonal changes might not occur in

neonates, due to immaturity in the secretion or signaling pathways of these hormones. In parallel, data from mouse models with activation of HIF1 pathway in β-cells showed varied consequences on glucose homeostasis, from mild adult hypoglycemia to impaired glucose tolerance and hyperglycemia, depending of Cre recombination driver used (12-15). Together these findings suggest that hypoxia and HIF1A pathway activation may have a similar impact on β-cell function in the early perinatal period and in adulthood.

We observed an impact of HIF1 pathway activation on the postnatal β-cell proliferation. The proliferation of islet cells peaks in rodents during the first week of life, then gradually decreases (44, 45). A similar pattern of proliferation occurs in children although the timeline is more prolonged, with significant β-cell proliferation until at least age 5 (46-48). This early postnatal proliferation wave in both rodents and humans establishes the adult β-cell mass. Any factor that impacts this period of proliferation may lead to a β-cell mass that is inadequate to sustain normal long-term glucose homeostasis. We have shown here that activation of HIF1A pathway in this early critical period leads to a dramatic decrease in replication and cell-cycle related transcripts, and to a decrease in the number of proliferating β-cells. This finding is intriguing but not surprising. β-cell insults in the prenatal period, such as those causing intrauterine growth restriction, lead to a significantly higher risk of diabetes in adulthood, at least in part due to a decreased β-cell mass (49-51). Decreased placental blood flow can diminish both nutrient and oxygen supplies to the fetus. The perinatal or postnatal consequences of hypoxia are also difficult to fully evaluate clinically in medically fragile newborns. Currently, long-term evaluation of children with perinatal stress-induced hyperinsulinism is not routinely performed. Additionally, survivors of childhood cyanotic heart diseases inducing hypoxia have an increased risk of diabetes, in the setting of normal adult weight (52). Together, these data suggest that hypoxia occurring during early postnatal period has long-term consequences by impacting postnatal β-cell mass expansion. We suggest that the underlying mechanism is a

direct role of HIF1A in antagonizing MYC transcriptional activity, as shown in other cell types (33).

In conclusion, pharmacologic or hypoxia-driven activation of HIF pathway in early postnatal period leads to hypoglycemia and hyperinsulinism, and impacts β-cell replication. This work establishes important models for the future investigation of the mechanism underlying perinatal stress-induced hyperinsulinism. These findings support the further investigation of the consequences of hypoxia on long-term glucose homeostasis, in both rodent models and in children.

Acknowledgements and funding: We thank Drs. Doris Stoffers and Ernestina Schipani for critical review of the manuscript. CAS was supported by NIH grant R37-DK056268. TH was supported in part by NIH DK098517. KJW was supported by Novo Nordisk Foundation NNF17CC0027852.

Data availability statement: whole islet transcriptomic data will be available upon request from DES.

Author contributions: JY, BH designed and performed experiments, interpreted the results with input from DES and wrote parts of the manuscript. AR performed experiments, wrote and revised the manuscript. AMA contributed to supervision of the project, experimental design, and edited/revised the manuscript. KJW supported the bioinformatic analysis and revised the manuscript. TH contributed to experimental design, interpreted the data and wrote/edited the manuscript. CAH conceptualized the project, wrote and edited the manuscript. DES conceptualized and supervised the project overall, analyzed the data, wrote/edited the manuscript.

Figure Legends

Figure 1: Inhibition of prolyl hydroxylases by Adaptaquin (AQ) leads to activation of the HIF1A pathway in rat islets. (A) Islets from AQ-treated P11 pups show higher levels of HIF1A: representative immunofluorescence images of islets for HIF1A (red), INS (green) and DAPI (blue) for each condition. (B) Islets from AQ-treated P11 pups show increased expression of HIF1A pathway targets by quantitative RT-PCR. **p*-value <0.005, ***p*-value=0.02

Figure 2: Early postnatal AQ-treatment leads to hyperinsulinism through decreased glucose threshold for insulin release. P11 rat pups that have been treated for 4 days (P7-P10) with AQ have lower body weights (A), lower random plasma glucose (B), higher serum insulin (C), and moderately higher serum glucagon (D). Correlation plots between plasma glucose and serum insulin (E) and glucose with glucagon (F) in individual animals. (G) Islet perifusions with stepwise increasing concentrations of glucose from 3 to 25 mM followed by 30 mM KCl show a left shift in the glucose threshold from 10 mM in control P11 pups to 5 mM in AQ-treated P11 pups. Insulin release per min is calculated as percentages of maximal KCl-stimulated insulin release for each replicate, from 200-250 islets/replicate/condition. n=3 independent pools of islets were obtained from 1-5 animals for each age. (H) Area under the curve of average insulin release, in P11 control and AQ-treated islets. Error bars represent SEM. *p*-values for A-D were calculated using unpaired t-test with Welch's correction. The data points were connected by straight lines for visual clarity only.

Figure 3: Activation of HIF1A pathway by AQ changes rat islet morphology. (A) AQ-treated pups have an overall larger insulin positive area per entire pancreas area. (B-E) Individual islets from AQ-treated pups show a higher average insulin area/cell (B) and higher average glucagon + areas per cell (C), but no change in the number of INS+ or GCG+ cells per islet (D-E). (F) Insulin content per pancreas weight, (G) Glucagon content per pancreas weight. For A, each

point represents an average measurement from 1 pup. For B-E, each point represents measurements of one islet, from 3 controls and 3 AQ-treated pups. p-values as depicted on the figures, calculated using Welch t-test (A, F, G) or Mann-Whitney test (B-E). INS = insulin. GCG = glucagon.

Figure 4: Activation of HIF1A pathway by AQ leads to broad changes in rat whole islet transcripts. (A) Canonical pathways altered in P11 AQ-treated islets compared to control, represented by -log(p-value). Pathways are labeled based on predicted directionality: green labels pathways predicted to be downregulated, red labels pathways predicted to be upregulated, gray labels pathway for which a directionality cannot be established in Ingenuity IPA. Activation/inhibition Z-scores (calculated in Ingenuity IPA) are specified for some pathways. (B) Selected differentially expressed transcripts in AQ-treated vs control pups.

Figure 5: Activation of HIF1A pathway by AQ leads to decreased β-cell proliferation. (A) Alteration of cell cycle-related transcripts in AQ-treated islets. (B) Two representative images of islets stained with INS (green), KI67 (red), and DAPI (blue) show markedly decreased β-cell proliferation. The white arrows indicate KI67+ β-cells. 20X magnification.

Supplemental data:

Supplemental Table 1 - Primers for RT-qPCR

Supplemental Table 2 - List of primary antibodies used for immunofluorescence

Supplemental Table 3 - Differential gene expression in whole islets from AQ-treated and control P11 pups.

Supplemental Figure 1: Inhibition of prolyl hydroxylases by AQ between P3-P7 leads to a lower body weight (A), lower plasma glucose (B), higher serum insulin (C). (D) Islet perifusions with increasing concentrations of glucose from 3-25 mM followed by depolarization with KCl (30 mM) shows a left shift in glucose threshold for insulin secretion in AQ-treated P7 pups compared to controls. (E) Area under the curve of average insulin release, in control and AQ-treated P7 islets.

Supplemental Figure 2: Perinatal hypoxia leads to hyperinsulinism due to decreased glucose threshold for insulin secretion. (A) Mice pups delivered in hypoxia have lower weights and plasma glucose and higher serum insulin and glucagon compared to mouse pups kept in room air. (B) Islet perifusions with increasing concentrations of glucose show a left shift in the glucose threshold for GSIS from 5 mM in normoxic P6 mouse pups to 3 mM in hypoxic P6 mouse pups. (C) Hypoxia leads to upregulation of HIF1A pathway targets in islets by quantitative RT qPCR

Supplemental Figure 3: Transcriptomic changes in islets from P11 AQ-treated pups vs control. (A) upregulation of hypoxia or HIF1A target genes. (B) no changes in expression of several known islet specific transcripts.

Supplemental Figure 4: (A) Brdu incorporation in islet cells from control and AQ-treated P11 rat pups – representative images of islets at 20x or 40x magnification. (B) network of upregulated (red) or downregulated (green) transcripts in islets from AQ-treated P11 pups that are downstream of MYC or E2F1.

References:

1. Pallotto EK WB, Simmons R, Macones GA. #47 Small for gestational age infants at risk for prolonged hypoglycemia. *Ann Epidemiol.* 2002;12(7):1.
2. Mizumoto H, Uchio H, Yamashita S, and Hata D. Transient neonatal hyperinsulinism with adaptation disorders: a report of three cases. *J Pediatr Endocrinol Metab.* 2015;28(3-4):337-40.
3. Hoe FM, Thornton PS, Wanner LA, Steinkrauss L, Simmons RA, and Stanley CA. Clinical features and insulin regulation in infants with a syndrome of prolonged neonatal hyperinsulinism. *J Pediatr.* 2006;148(2):207-12.
4. Lord K, and De Leon DD. Hyperinsulinism in the Neonate. *Clin Perinatol.* 2018;45(1):61-74.
5. McKinlay CJD, Alsweiler JM, Anstice NS, Burakevych N, Chakraborty A, Chase JG, et al. Association of Neonatal Glycemia With Neurodevelopmental Outcomes at 4.5 Years. *JAMA Pediatr.* 2017;171(10):972-83.
6. Semenza GL. Hypoxia-inducible factor 1: control of oxygen homeostasis in health and disease. *Pediatr Res.* 2001;49(5):614-7.
7. Salceda S, and Caro J. Hypoxia-inducible factor 1α (HIF-1α) protein is rapidly degraded by the ubiquitin-proteasome system under normoxic conditions. Its stabilization by hypoxia depends on redox-induced changes. *J Biol Chem.* 1997;272(36):22642-7.
8. Shah SR, Esni F, Jakub A, Paredes J, Lath N, Malek M, et al. Embryonic mouse blood flow and oxygen correlate with early pancreatic differentiation. *Dev Biol.* 2011;349(2):342-9.
9. Zeng C, Mulas F, Sui Y, Guan T, Miller N, Tan Y, et al. Pseudotemporal Ordering of Single Cells Reveals Metabolic Control of Postnatal β Cell Proliferation. *Cell Metab.* 2017;25(5):1160-75 e11.

10. Heinis M, Simon MT, Ilc K, Mazure NM, Pouyssegur J, Scharfmann R, et al. Oxygen tension regulates pancreatic β-cell differentiation through hypoxia-inducible factor 1α. *Diabetes.* 2010;59(3):662-9.

11. Puri S, Garcia-Nunez A, Hebrok M, and Cano DA. Elimination of von Hippel-Lindau function perturbs pancreas endocrine homeostasis in mice. *PLoS One.* 2013;8(8):e72213.

12. Zehetner J, Danzer C, Collins S, Eckhardt K, Gerber PA, Ballschmieter P, et al. PVHL is a regulator of glucose metabolism and insulin secretion in pancreatic β cells. *Genes Dev.* 2008;22(22):3135-46.

13. Cantley J, Selman C, Shukla D, Abramov AY, Forstreuter F, Esteban MA, et al. Deletion of the von Hippel-Lindau gene in pancreatic β cells impairs glucose homeostasis in mice. *J Clin Invest.* 2009;119(1):125-35.

14. Shen HC, Adem A, Ylaya K, Wilson A, He M, Lorang D, et al. Deciphering von Hippel-Lindau (VHL/Vhl)-associated pancreatic manifestations by inactivating Vhl in specific pancreatic cell populations. *PLoS One.* 2009;4(4):e4897.

15. Puri S, Cano DA, and Hebrok M. A role for von Hippel-Lindau protein in pancreatic β-cell function. *Diabetes.* 2009;58(2):433-41.

16. Yang J, Hammoud B, Li C, Ridler A, Yau D, Kim J, et al. Decreased KATP channel activity contributes to the low glucose threshold for insulin secretion in the early postnatal period. *bioRxiv.* 2021:2021.03.04.433947.

17. Anders S, and Huber W. Differential expression analysis for sequence count data. *Genome Biol.* 2010;11(10):R106.

18. Karuppagounder SS, Alim I, Khim SJ, Bourassa MW, Sleiman SF, John R, et al. Therapeutic targeting of oxygen-sensing prolyl hydroxylases abrogates ATF4-dependent neuronal death and improves outcomes after brain hemorrhage in several rodent models. *Sci Transl Med.* 2016;8(328):328ra29.

19. Fraisl P, Aragones J, and Carmeliet P. Inhibition of oxygen sensors as a therapeutic strategy for ischaemic and inflammatory disease. *Nat Rev Drug Discov.* 2009;8(2):139-52.

20. O'Reilly SM, Leonard MO, Kieran N, Comerford KM, Cummins E, Pouliot M, et al. Hypoxia induces epithelial amphiregulin gene expression in a CREB-dependent manner. *Am J Physiol Cell Physiol.* 2006;290(2):C592-600.

21. Yamaguchi J, Tanaka T, Eto N, and Nangaku M. Inflammation and hypoxia linked to renal injury by CCAAT/enhancer-binding protein delta. *Kidney Int.* 2015;88(2):262-75.

22. Tanaka T, Wiesener M, Bernhardt W, Eckardt KU, and Warnecke C. The human HIF (hypoxia-inducible factor)-3α gene is a HIF-1 target gene and may modulate hypoxic gene induction. *Biochem J.* 2009;424(1):143-51.

23. Hernandez C, Santamatilde E, McCreath KJ, Cervera AM, Diez I, Ortiz-Masia D, et al. Induction of trefoil factor (TFF)1, TFF2 and TFF3 by hypoxia is mediated by hypoxia inducible factor-1: implications for gastric mucosal healing. *Br J Pharmacol.* 2009;156(2):262-72.

24. Furuta GT, Turner JR, Taylor CT, Hershberg RM, Comerford K, Narravula S, et al. Hypoxia-inducible factor 1-dependent induction of intestinal trefoil factor protects barrier function during hypoxia. *J Exp Med.* 2001;193(9):1027-34.

25. Li X, Lee Y, Kang Y, Dai B, Perez MR, Pratt M, et al. Hypoxia-induced autophagy of stellate cells inhibits expression and secretion of lumican into microenvironment of pancreatic ductal adenocarcinoma. *Cell Death Differ.* 2019;26(2):382-93.

26. Liu M, Zhang L, Marsboom G, Jambusaria A, Xiong S, Toth PT, et al. Sox17 is required for endothelial regeneration following inflammation-induced vascular injury. *Nat Commun.* 2019;10(1):2126.

27. Jonatan D, Spence JR, Method AM, Kofron M, Sinagoga K, Haataja L, et al. Sox17 regulates insulin secretion in the normal and pathologic mouse β cell. *PLoS One.* 2014;9(8):e104675.

28. Neve B, Fernandez-Zapico ME, Ashkenazi-Katalan V, Dina C, Hamid YH, Joly E, et al. Role of transcription factor KLF11 and its diabetes-associated gene variants in pancreatic β cell function. *Proc Natl Acad Sci U S A.* 2005;102(13):4807-12.

29. Ushijima K, Narumi S, Ogata T, Yokota I, Sugihara S, Kaname T, et al. KLF11 variant in a family clinically diagnosed with early childhood-onset type 1B diabetes. *Pediatr Diabetes.* 2019;20(6):712-9.

30. Gutierrez GD, Bender AS, Cirulli V, Mastracci TL, Kelly SM, Tsirigos A, et al. Pancreatic β cell identity requires continual repression of non-β cell programs. *J Clin Invest.* 2017;127(1):244-59.

31. Taylor BL, Liu FF, and Sander M. Nkx6.1 is essential for maintaining the functional state of pancreatic β cells. *Cell Rep.* 2013;4(6):1262-75.

32. Zhang H, Ackermann AM, Gusarova GA, Lowe D, Feng X, Kopsombut UG, et al. The FoxM1 transcription factor is required to maintain pancreatic β-cell mass. *Mol Endocrinol.* 2006;20(8):1853-66.

33. Koshiji M, Kageyama Y, Pete EA, Horikawa I, Barrett JC, and Huang LE. HIF-1α induces cell cycle arrest by functionally counteracting Myc. *EMBO J.* 2004;23(9):1949-56.

34. Blum B, Hrvatin S, Schuetz C, Bonal C, Rezania A, and Melton DA. Functional β-cell maturation is marked by an increased glucose threshold and by expression of urocortin 3. *Nat Biotechnol.* 2012;30(3):261-4.

35. Henquin JC, and Nenquin M. Immaturity of insulin secretion by pancreatic islets isolated from one human neonate. *J Diabetes Investig.* 2018;9(2):270-3.

36. Gelling RW, Du XQ, Dichmann DS, Romer J, Huang H, Cui L, et al. Lower blood glucose, hyperglucagonemia, and pancreatic α cell hyperplasia in glucagon receptor knockout mice. *Proc Natl Acad Sci U S A.* 2003;100(3):1438-43.

37. Hancock AS, Du A, Liu J, Miller M, and May CL. Glucagon deficiency reduces hepatic glucose production and improves glucose tolerance in adult mice. *Mol Endocrinol.* 2010;24(8):1605-14.

38. Huang C, Walker EM, Dadi PK, Hu R, Xu Y, Zhang W, et al. Synaptotagmin 4 Regulates Pancreatic β Cell Maturation by Modulating the Ca(2+) Sensitivity of Insulin Secretion Vesicles. *Dev Cell.* 2018;45(3):347-61 e5.

39. Sekine N, Cirulli V, Regazzi R, Brown LJ, Gine E, Tamarit-Rodriguez J, et al. Low lactate dehydrogenase and high mitochondrial glycerol phosphate dehydrogenase in pancreatic β-cells. Potential role in nutrient sensing. *J Biol Chem.* 1994;269(7):4895-902.

40. Pullen TJ, Khan AM, Barton G, Butcher SA, Sun G, and Rutter GA. Identification of genes selectively disallowed in the pancreatic islet. *Islets.* 2010;2(2):89-95.

41. Thorrez L, Laudadio I, Van Deun K, Quintens R, Hendrickx N, Granvik M, et al. Tissue-specific disallowance of housekeeping genes: the other face of cell differentiation. *Genome Res.* 2011;21(1):95-105.

42. Oltmanns KM, Gehring H, Rudolf S, Schultes B, Rook S, Schweiger U, et al. Hypoxia causes glucose intolerance in humans. *Am J Respir Crit Care Med.* 2004;169(11):1231-7.

43. Punjabi NM, Sorkin JD, Katzel LI, Goldberg AP, Schwartz AR, and Smith PL. Sleep-disordered breathing and insulin resistance in middle-aged and overweight men. *Am J Respir Crit Care Med.* 2002;165(5):677-82.

44. Finegood DT, Scaglia L, and Bonner-Weir S. Dynamics of β-cell mass in the growing rat pancreas. Estimation with a simple mathematical model. *Diabetes.* 1995;44(3):249-56.

45. Qiu WL, Zhang YW, Feng Y, Li LC, Yang L, and Xu CR. Deciphering Pancreatic Islet β Cell and α Cell Maturation Pathways and Characteristic Features at the Single-Cell Level. *Cell Metab.* 2017;25(5):1194-205 e4.

46. Gregg BE, Moore PC, Demozay D, Hall BA, Li M, Husain A, et al. Formation of a human β-cell population within pancreatic islets is set early in life. *J Clin Endocrinol Metab.* 2012;97(9):3197-206.

47. Wang P, Fiaschi-Taesch NM, Vasavada RC, Scott DK, Garcia-Ocana A, and Stewart AF. Diabetes mellitus--advances and challenges in human β-cell proliferation. *Nat Rev Endocrinol.* 2015;11(4):201-12.

48. Meier JJ, Butler AE, Saisho Y, Monchamp T, Galasso R, Bhushan A, et al. β-cell replication is the primary mechanism subserving the postnatal expansion of β-cell mass in humans. *Diabetes.* 2008;57(6):1584-94.

49. Van Assche FA, De Prins F, Aerts L, and Verjans M. The endocrine pancreas in small-for-dates infants. *Br J Obstet Gynaecol.* 1977;84(10):751-3.

50. Limesand SW, Jensen J, Hutton JC, and Hay WW, Jr. Diminished β-cell replication contributes to reduced β-cell mass in fetal sheep with intrauterine growth restriction. *Am J Physiol Regul Integr Comp Physiol.* 2005;288(5):R1297-305.

51. Simmons RA, Templeton LJ, and Gertz SJ. Intrauterine growth retardation leads to the development of type 2 diabetes in the rat. *Diabetes.* 2001;50(10):2279-86.

52. Madsen NL, Marino BS, Woo JG, Thomsen RW, Videboek J, Laursen HB, et al. Congenital Heart Disease With and Without Cyanotic Potential and the Long-term Risk of Diabetes Mellitus: A Population-Based Follow-up Study. *J Am Heart Assoc.* 2016;5(7).

Figure 1

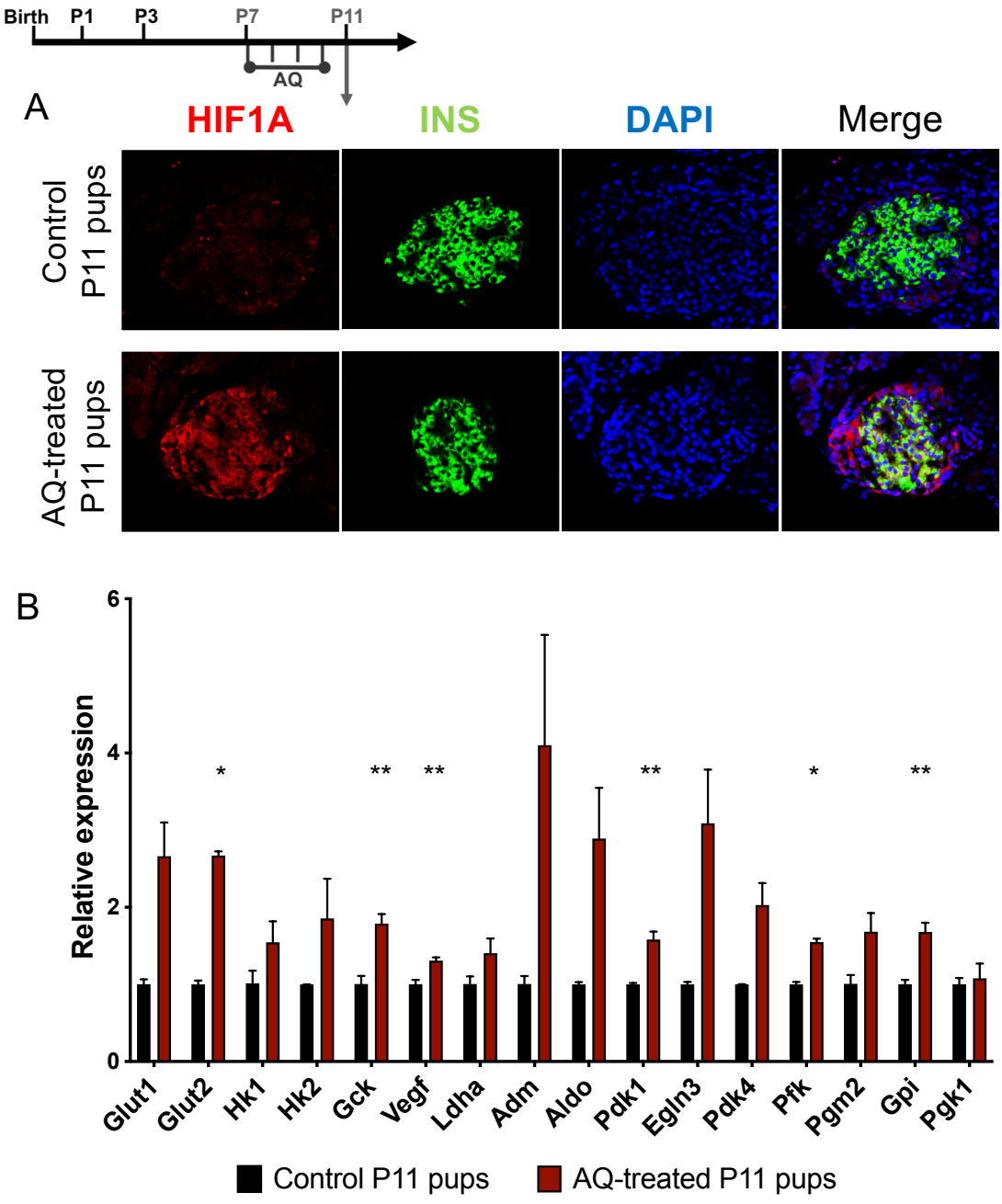

Figure 2

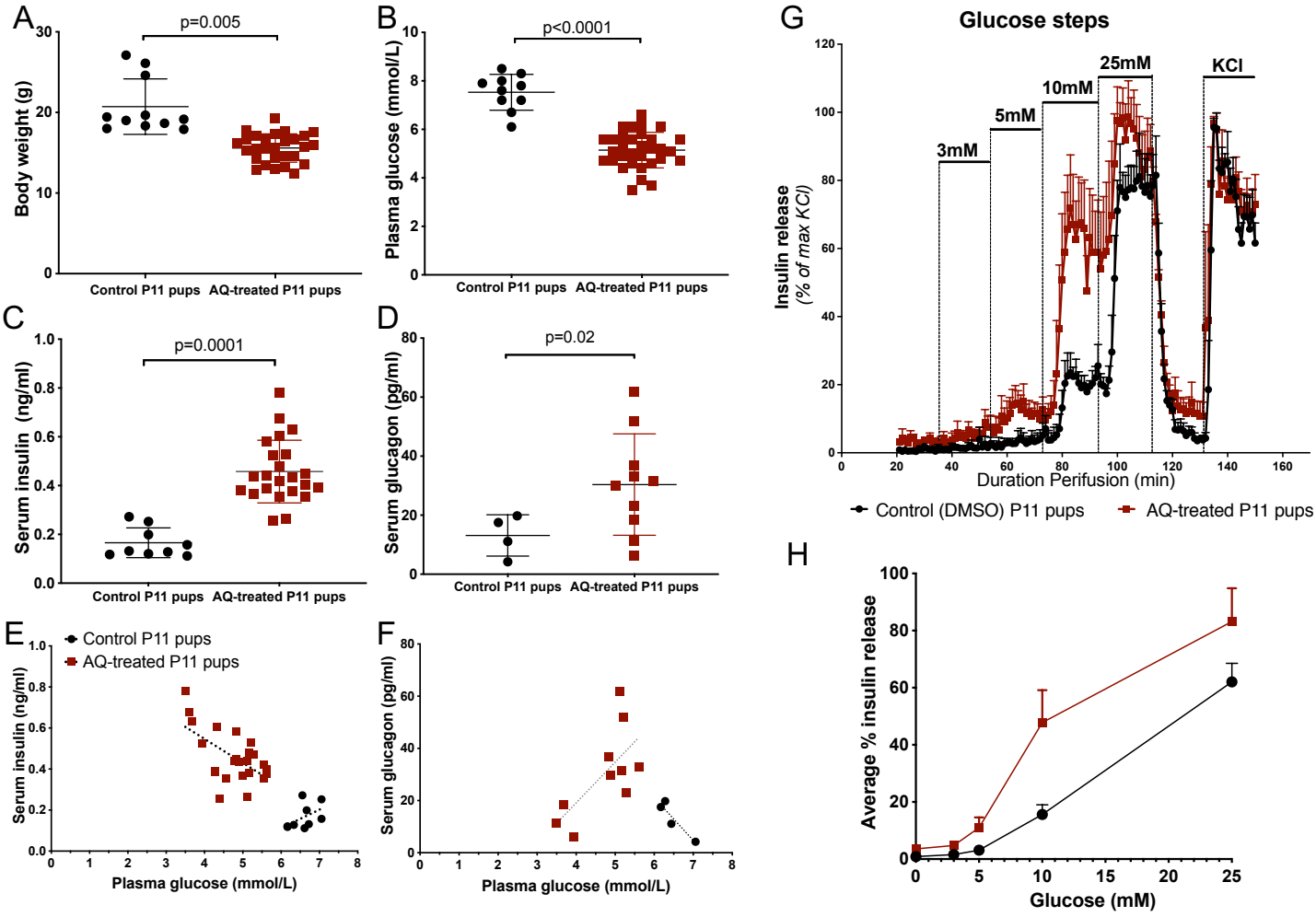

Figure 3

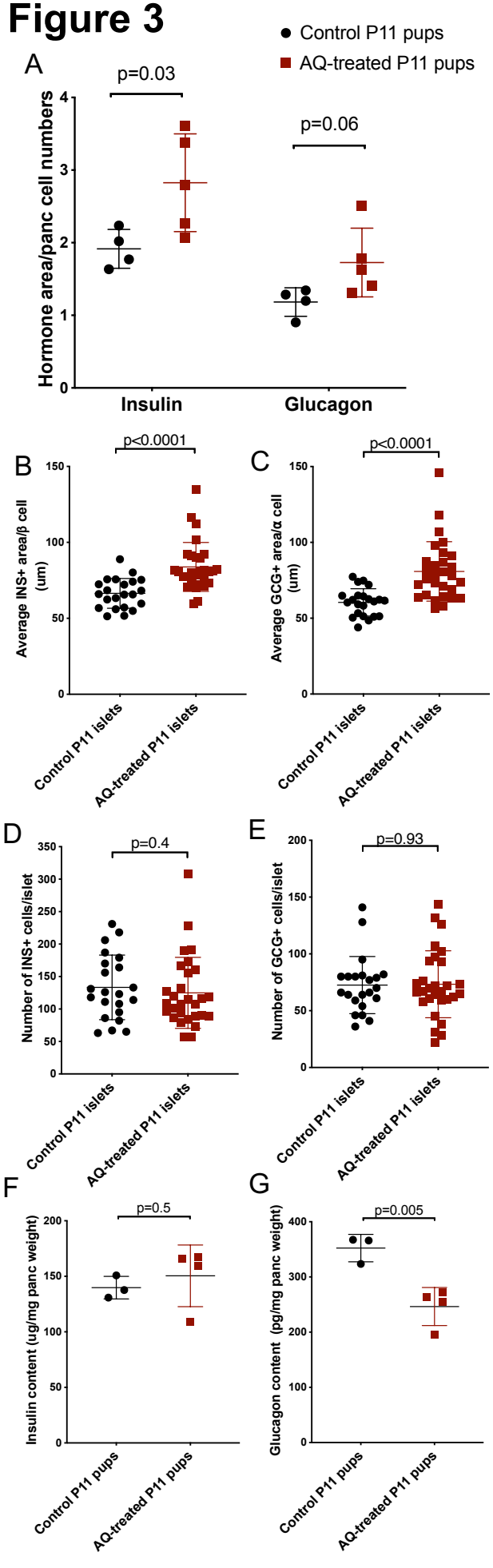

Figure 4

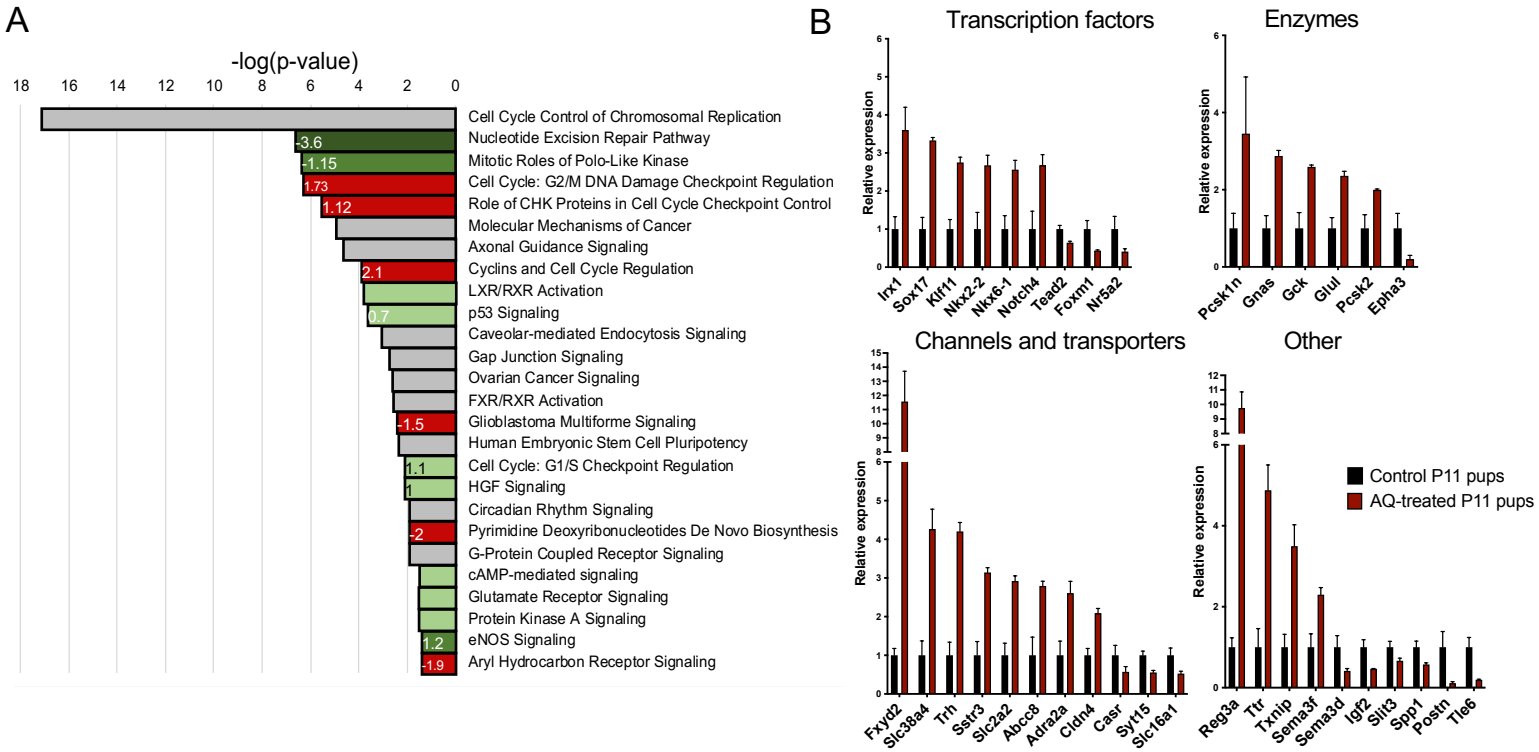

Figure 5

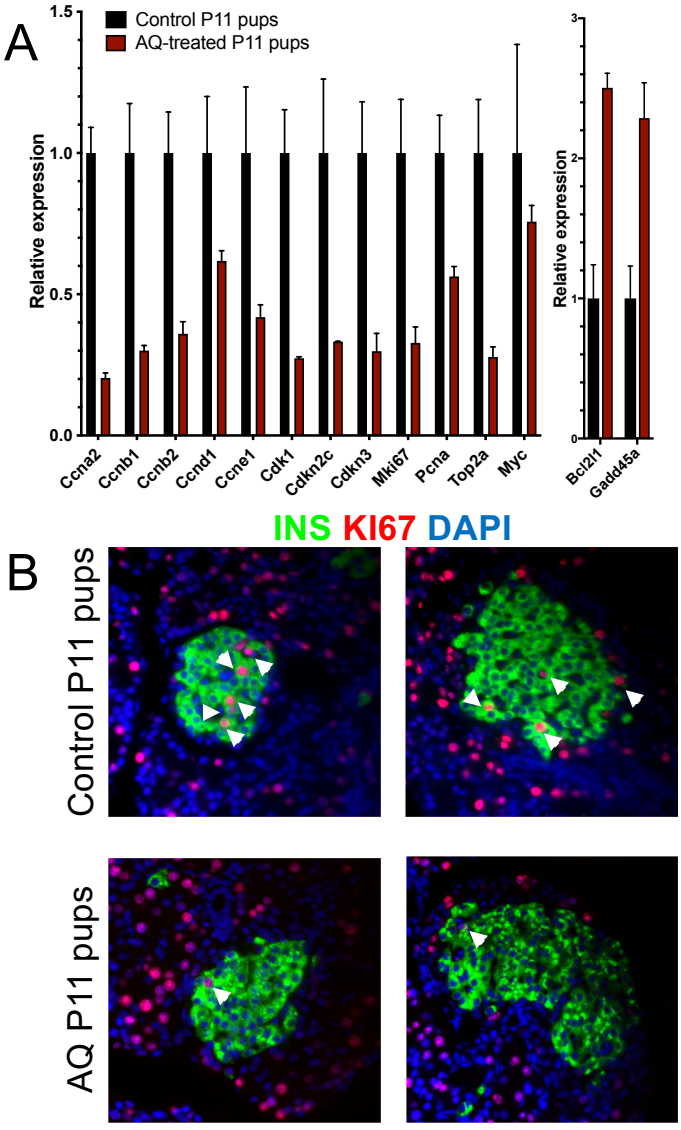

Supplemental Figure 1

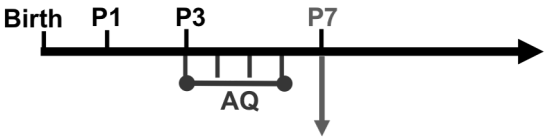

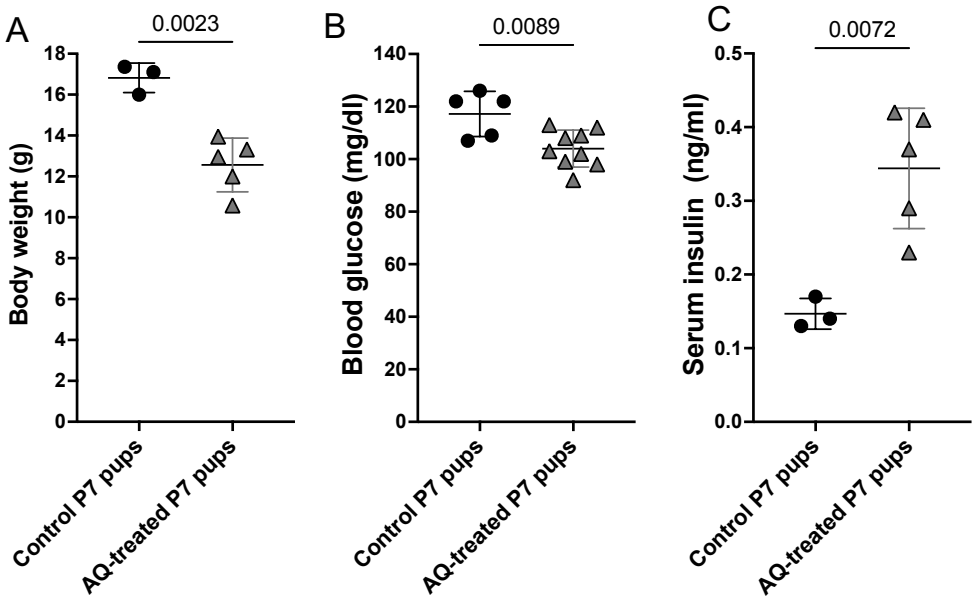

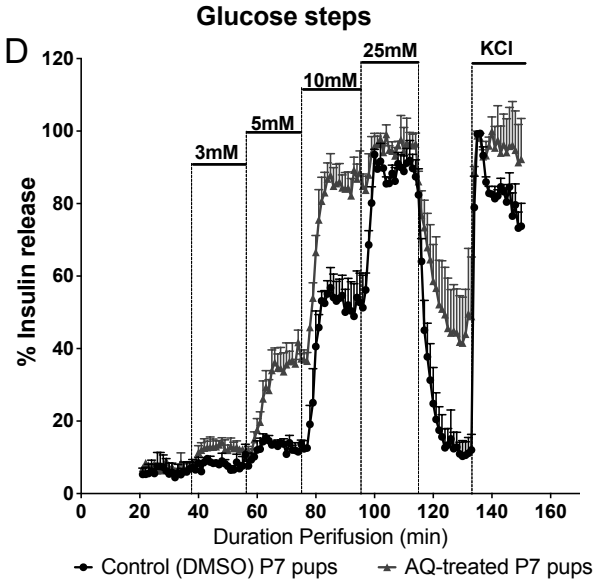

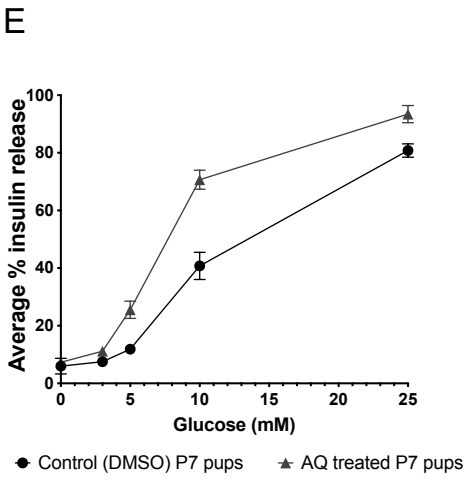

Supplemental Figure 2

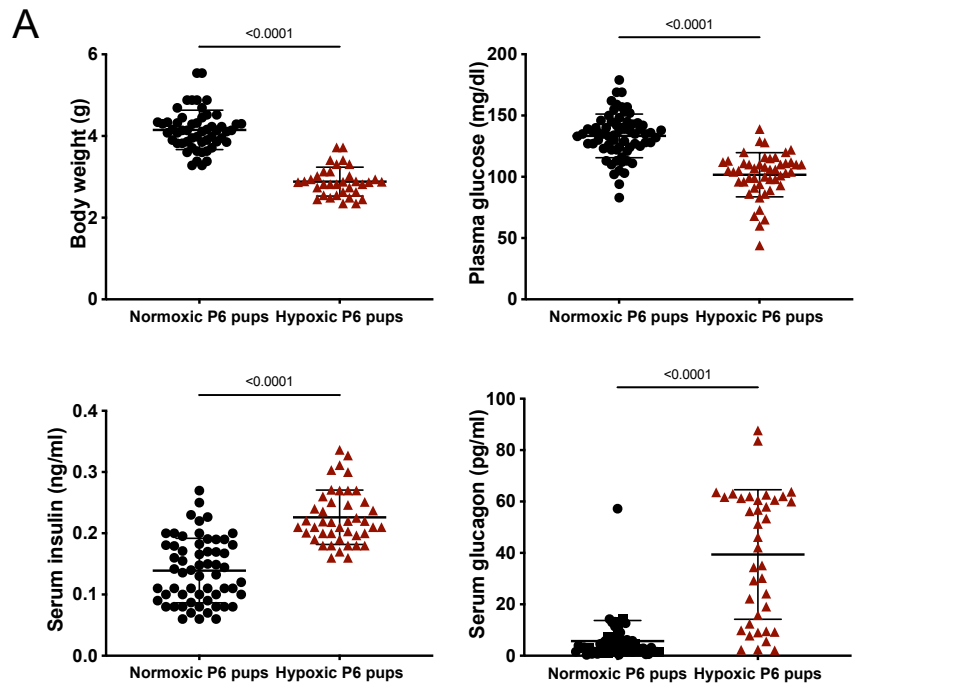

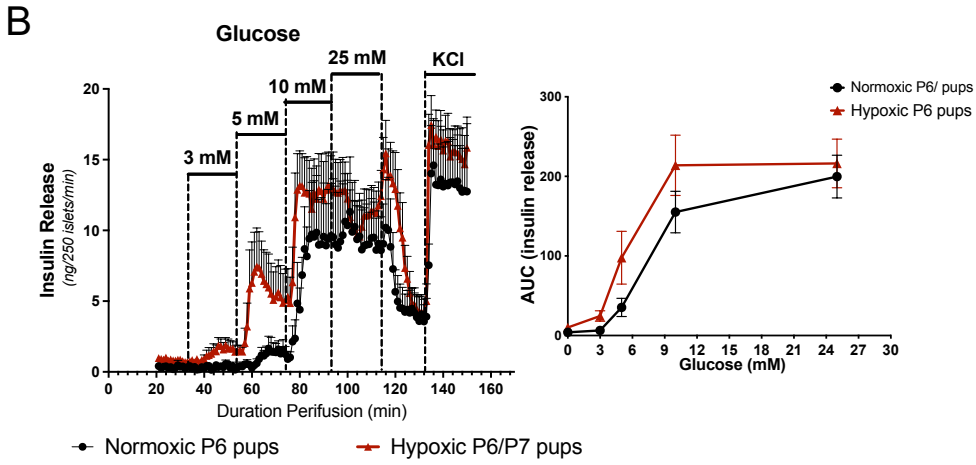

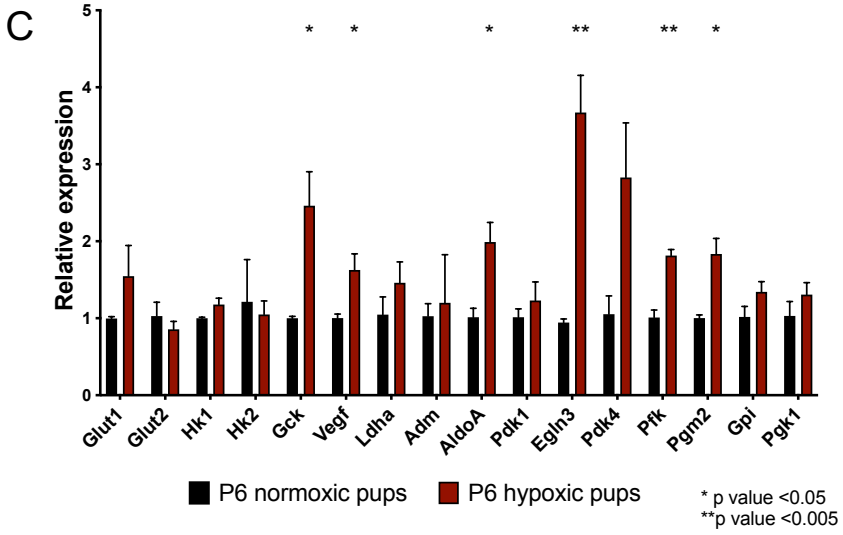

Supplemental Figure 3

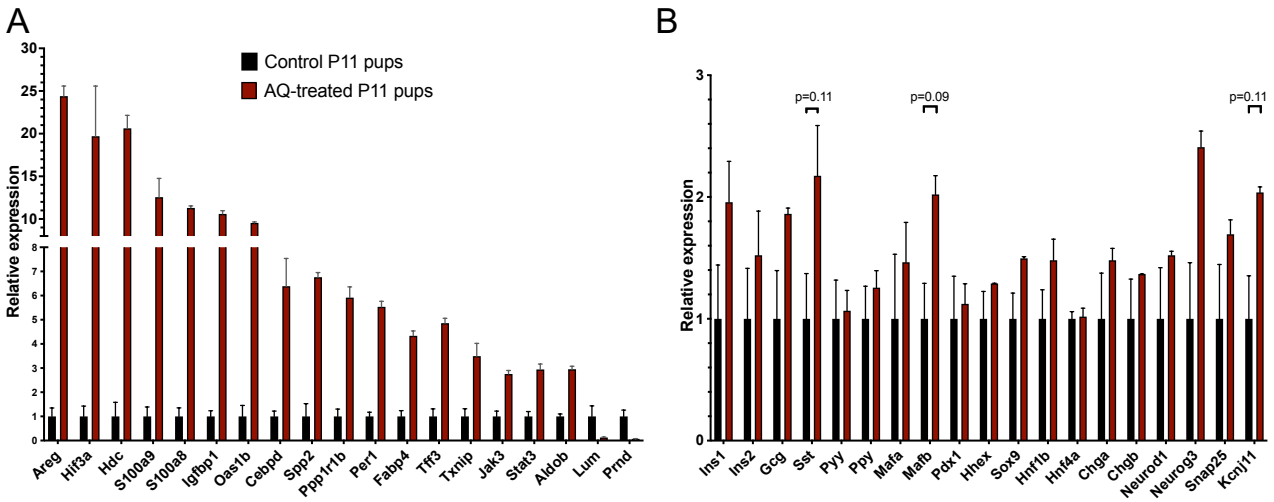

Supplemental figure 4

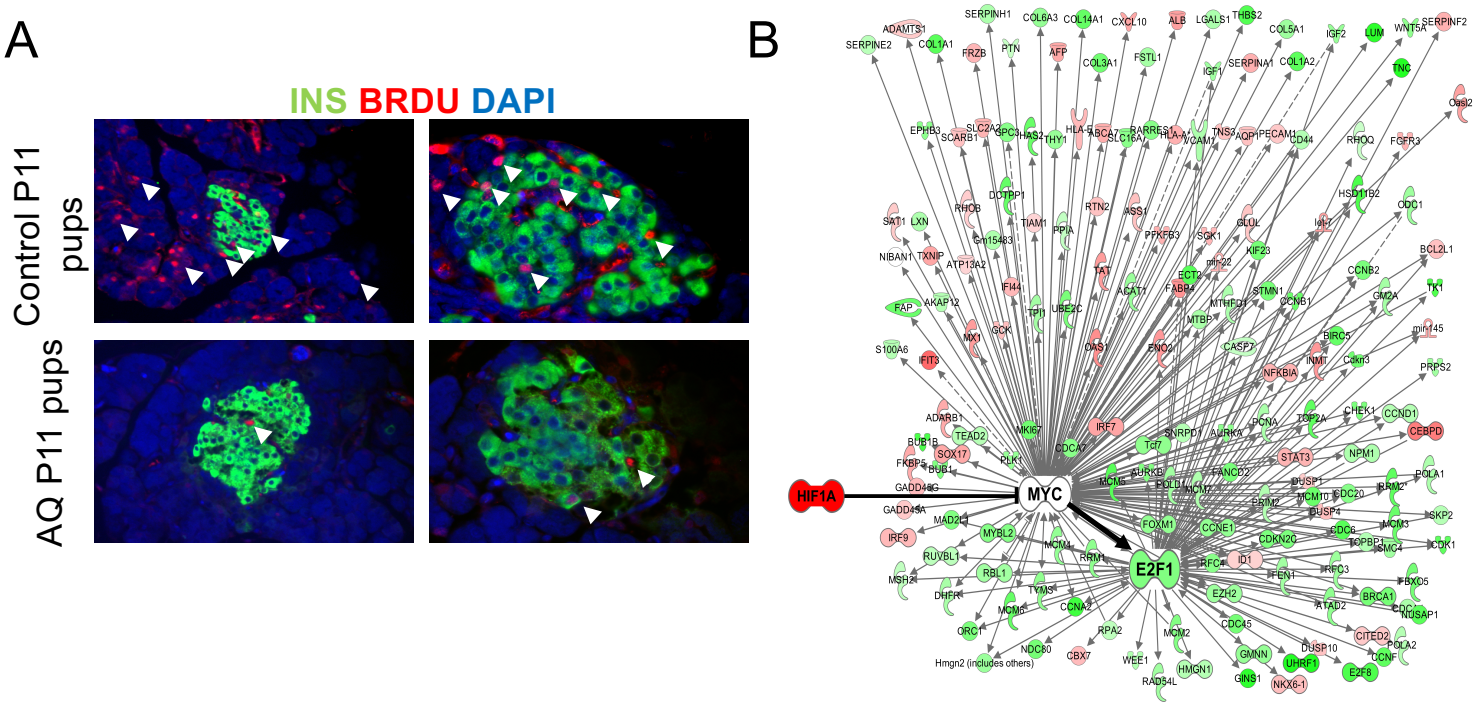

Supplemental Table 1

List of Primer sequences used for Quantitative PCR

Rat

Genes	Forward primer sequences (5' to 3')	Reverse primer sequences (5' to 3')
Glut1	TTGCTGCAGAATTCCGGAAG	AGCTCATCCTCACACAGTCT
Glut2	CAAACTGACAGATCTCGGGC	TGGAGCCATCAAAGTCCTGA
HK1	GTGACGACAGTATCCTGGTCAA	ACACGGTACACTTTGGTGACAG
HK2	CACTGTGAAGTTGGCCTCATTG	ATCCACAGCAACATCAAACACG
GCK	GCCCAGTGAAATCCAGGTCA	GGGGTAGCAGCAGAATAGGT
Vegf	TTGCAGATGTGACAAGCCAA	GTCTTTCCGGTGAGAGGTCT
Ldha	TCCTCAGCGTCCCATGTATC	TCTGCACTCTTCTTCAGGCG
Adm	GCAGACACACTCAGCTCCA	TACTCGCCCGACTGTTCAAT
Aldo	CAGTATGTTCACACGGGCTC	GCTGGTAGGTGACGGTATCT
Pdk1	CTCACAGAAGGGCCACATTT	GCTTCTGGTCGGAGTTCTTG
Egln3	GCTTGCTATCCAGGAAATGG	TGGCGTCCCAATTCTTATTC
Pdk4	AGTTCTGAGGCTGATGACTGG	GACCCACTTTGATCCCGTAA
Pfk	CTTACCGATCACCCTCGTTC	GCTCCGAGTTCCATGTGAGT
Pgm2	TCCAGCCACAAAAGTATAACCT	TCAAGTTCAGCCTAATTGGAG
Gpi	CCTCCACTAATGGACTGATCG	GAAGGGACACGAAGTCAGGA
Pgk1	TGGATGCTCTCAGCAATGTT	CAAATGGAGATGCGGAAAAC
Actin	CCTCATGAAGATCCTGACCGAG	AGTTTCATGGATGCCACAGGAT

Mouse

Genes	Forward primer sequences (5' to 3')	Reverse primer sequences (5' to 3')
Glut1	TTGCTGCAGAATTCCGGAAG	AGCTCATCCTCACACAGTCT
Glut2	CAAACTGACAGATCTCGGGC	TGGAGCCATCAAAGTCCTGA
HK1	CAGATCGAGAGTGACCGATTAG	AGTGTGGATGGAGTTTGTAGAG
HK2	GCTGCTGGAGGTTAAGAGAAG	CTGGAGTGGCACACACATAA
GCK	GAAATCCAGGAGATGCCAGA	GAAGCTGCCATCCTGCTAAC
Vegf	TTGCAGATGTGACAAGCCAA	GTCTTTCCGGTGAGAGGTCT
Ldha	TCCTCAGCGTCCCATGTATC	TCTGCACTCTTCTTCAGGCG
Adm	CCTGCGGAATCAGAGAACTT	GCTTGGTCTTGGGTTCCTCT
Aldo	CCTCGCTTGTCAAGGAAAGT	TGGAGCAGCCTTAGTTCAGC
Pdk1	CTCACAGAAGGGCCACATTT	GCTTCTGGTCGGAGTTCTTG
Egln3	GCTTGCTATCCAGGAAATGG	TGGCGTCCCAATTCTTATTC
Pdk4	CACAAAACCAAGCAAGCAAA	GACACCTGTTATCCCCTGGA
Pfk	GCATAGACAAGGGTTTCTGAGC	TCCCGAGTTCCCCTTGAGTT
Pgm2	TTGAAGAGCACGGACAGAAA	AGTGCCTCACAAATGGCTGT
Gpi	CCTCCACTAATGGACTGATCG	GAAGGGACACGAAGTCAGGA
Pgk1	TGGATGCTCTCAGCAATGTT	CAAATGGAGATGCGGAAAAC
Actin	CTGTCCCTGTATGCCTCTG	ATGTCACGCACGATTTCC

Supplemental Table 2

Target	Raised in	Concentration	Source
Insulin	Mouse (McAb)		Proteintech (Cat no. 66198-1- Ig)
	Rabbit (PolyAb)		Proteintech (Cat no. 15848-1-AP)
Glucagon	Mouse (mAb)		Abcam (Cat no. ab82270)
	Rabbit (PolyAb)		Proteintech (Cat no. 15954-1-AP)
HIF1A	Rabbit	1:500	Invitrogen (Cat no. PA1-16627)
KI67	Rabbit	1:200	Abcam (Cat no. ab15580)
BRDU	Rat	1:500	Abcam (Cat no. ab6326)